

Unified treatment of temperature, concentration, and electric-field dependences of variable-range-hopping conductivity

X. X. Wang, C. J. Martoff, and E. Kaczanowicz

Physics Department, Temple University, Philadelphia, Pennsylvania 19122

(Received 15 July 1994; revised manuscript received 3 October 1994)

The conductivity of $\text{Ge}_{1-x}\text{Au}_x$ thin films was studied at temperatures in the range $0.019 < T < 4.2$ K. In the linear (low-bias) regime, samples with $0 < x < 0.14$ showed resistivity with $\exp \sqrt{T^*/T}$ behavior. The x dependence of T^* accurately followed the theory of Shklovskii and Efros, which includes a Coulomb gap in the electronic density of states. At bias fields exceeding $\sim 10^4$ V/m, nonlinearity was observed that can be accounted for by introducing the effect of the bias field into a calculation of the optimized hopping exponent.

I. INTRODUCTION

Variable-range hopping conductivity (VRHC) is an intrinsically interesting phenomenon that has been studied both experimentally and theoretically in recent years.¹⁻⁸ As a practical matter, VRHC is believed to be the mechanism of electrical conduction in neutron transmutation doped germanium (NTD-Ge) which is widely used for cryogenic thermometry.^{9,10} The present work was motivated by the desire to produce thin-film bolometers that could be directly deposited on radiation absorbers to act as ultralow-mass, high-sensitivity cryogenic microcalorimeters for detection of radiation interactions, specifically in connection with the search for weakly interacting particulate dark matter in the galaxy.^{11,12}

In the course of this research, we have studied a large number of thin-film GeAu samples on silicon wafers, measuring the temperature and bias dependence of their resistivity. The dependence upon temperature and Au concentration is found to be consistent in detail with the VRHC models originated by Mott¹³ and others,¹⁴ and further developed by Efros and Shklovskii.¹ It is also found that the effect of the bias electric field can be incorporated into this theory in a natural way, explaining the general character of the residual nonlinearity in the resistivity after self-heating is accounted for.

II. EXPERIMENT

GeAu thin films were prepared by filament evaporation in a diffusion pumped, LN_2 trapped bell jar system with base pressure 10^{-6} Torr. The evaporation rate was found to be an important process variable, and was controlled manually through the filament current. Substrates (n -type Si, > 1 $\text{K}\Omega\text{cm}$ and p -type Si, > 1.8 $\text{K}\Omega\text{cm}$) were not temperature controlled, but it was found by direct measurement that the substrate temperature did not rise above 35°C during the deposition. Most films studied were about 2000 Å thick.

Au electrode films ~ 700 Å thick were subsequently

were patterned photolithographically using a standard KI etchant, forming interdigitated structures designed to give devices with resistance ~ 1 –50 $\text{M}\Omega$ at the temperature of interest. The etchant was found not to attack the underlying GeAu film. The electrode structures had up to 256 fingers with GeAu gaps as small as 15 μm . Individual devices were 6×6 mm^2 .

Measurements were performed in several cryostats for the different temperature ranges studied. A versatile dip-probe for insertion into a LHe storage dewar was designed by one of us (E.K.), permitting measurements at 4.2 K or above with the sample in vacuum. This was mainly used for the rapid screening of samples before study at lower temperatures. A pumped- ^4He probe permitted studies down to 1.4 K. Measurements to 0.27 K were performed with a sealed, sorb-pumped ^3He cryostat designed by Neuhauser.¹⁵ The lowest temperature range studied was 19–50 mK, obtained with the Oxford dilution refrigerator at the U.C. Berkeley Center for Particle Astrophysics.

Four-terminal resistance was measured with standard low-noise voltmeters (Kiethley R491) and battery-operated bias sources.

III. RESULTS AND DISCUSSION

A. Low-bias region

Samples were studied over a wide range of Au concentrations, in order to obtain devices suitable for use at various temperatures. Figure 1 shows the low-bias resistivity of $\text{Ge}_{1-x}\text{Au}_x$ films with $0.016 < x < 0.135$. Some datasets terminate within the displayed temperature range because the sample resistance became too large to measure, even for the most highly interdigitated electrode configuration.

These results are consistent with the theory of weak localization and VRHC in the presence of a Coulomb gap (SE-VRHC).¹ In the limit of low bias, the resistivities closely followed

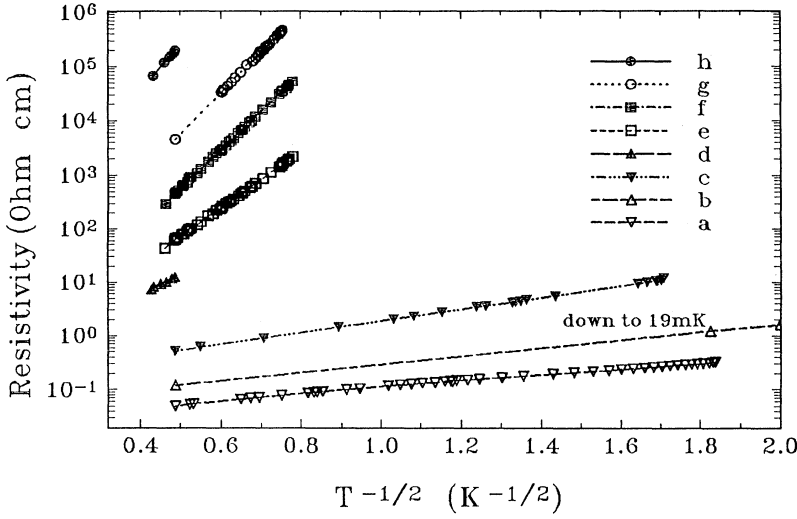


FIG. 1. The dependence relation of low-bias resistivity for thin-film Ge-Au samples having different Au concentrations.

$$\rho(T) = \rho_0 \exp \sqrt{\frac{T^*}{T}}. \quad (1)$$

A few samples with $x > 0.135$ stored in dry air for over six months, although initially following Eq. (1), changed after storage to a Mott-type VRH (M-VRHC) in which the power of temperature in the exponent is $1/4$ rather than $1/2$.¹⁶ Samples in this same concentration range stored in dry vacuum (~ 50 mTorr) for as long as a year, still followed the SE-VRHC behavior.

The dependence of T^* upon Au (impurity) concentration is predicted by the SE-VRHC model to be

$$T^* = \frac{2.88e^2}{k_b \kappa a}. \quad (2)$$

Here e is the electronic charge, a is the localization radius for the impurity wave function, k_b is Boltzmann's constant, and κ is the dielectric constant of the doped material.

This expression is obtained by optimization of the exponential factor governing the tunneling resistance of the current carrying electrons, using a method originated by Mott.¹³ The hopping (tunneling) resistance for two states i and j separated in position by r and in energy by ϵ is¹

$$R_{ij} = R_{ij}^0 \exp(2r_{ij}/a + \epsilon_{ij}/k_b T). \quad (3)$$

Mott's optimization procedure consists of minimizing the exponent with respect to r , taking into account the dependence of ϵ upon r . This dependence arises because as longer hops are considered, it is likely that a state with energy closer to the initial state can be found. For a density of states $g(\epsilon) = 3\kappa^3(\epsilon - E_F)^2/(\pi e^6)$ which vanishes quadratically at the Fermi energy (due to Coulomb repulsion of electrons in the heavily doped material¹), the number of states within an energy ϵ_0 of E_F is found to be $N(\epsilon_0) = 2\kappa^3 \epsilon_0^3/(\pi e^6)$. Given this number density, a radius r can be computed such that a sphere of radius r contains on average one state with a particular energy ϵ_0 . Inversion of the resulting formula for $r(\epsilon)$ gives the desired dependence of ϵ upon r for use in the optimiza-

tion. Minimizing the tunneling exponent with respect to r then yields a minimum (optimized) tunneling resistance

$$R_{ij} = R_{ij}^0 \exp(T^*/T)^{1/2} \quad (4)$$

with T^* given by Eq. (2) above.

If the density of states does not vanish at the Fermi level but is rather taken to be constant, the optimization procedure yields the M-VRHC expression in which $(T^*/T)^{1/4}$ replaces $(T^*/T)^{1/2}$, in Eq. (1) above, and T^* is given by

$$T_{\text{MVRHC}}^* = \frac{512}{9\pi g(E_F) a^3 k_b}. \quad (5)$$

The parameter T^* of Eq. (2) depends upon the impurity concentration implicitly through the dielectric constant κ . It is to be expected that κ would vary little from the standard Ge value of 16 until the impurity concentration becomes reasonably high, perhaps several atom percent. Very near the the insulator-to-metal transition (which in these films occurs above 13.6 atom percent Au), Mott¹⁶ has shown that the dielectric constant should increase with impurity concentration as a power law.

The present data are in good agreement with these expectations. Figure 2 shows the measured T^* and empirical fitting for T^* . The only fitted parameter in this analysis is the effective mass m^* , which is taken to be $0.16m_e$ rather than the standard value $0.12m_e$ for crystalline Ge. Using Eq. (2), we found that

$$\kappa a = \frac{\hbar^2}{m^* e^2} \left(\frac{13.65}{13.65 - x} 16.2 \right)^2. \quad (6)$$

We cannot determine the localization radius directly from our experimental data. However, from electric-field effects measurements (we will discuss it later), we found out that if the localization radius behaves like

$$a = \frac{\hbar^2}{m^* e^2} 16.2 \frac{13.65}{13.65 - x}, \quad (7)$$

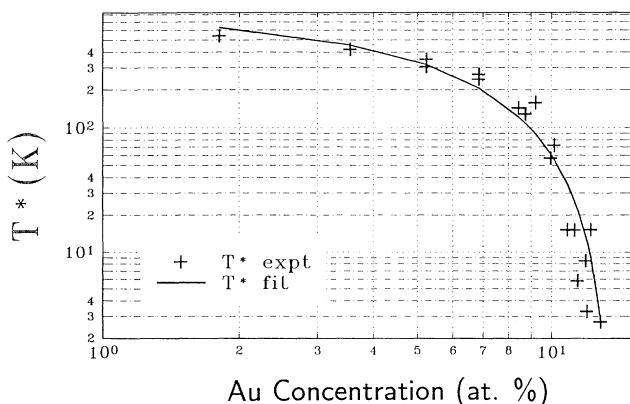


FIG. 2. Dependence of the SE-VRHC parameter T^* upon the Au concentration.

our experiment point can be fit with the expression of optimized electric-field-induced resistivity. If this is the case, using Eqs. (6) and (7), we obtained the dielectric constant κ as follows in Eq. (8). The calculated κ is close to 16 at low Au concentrations. At higher concentrations, the dependence is well fit by an empirical expression as shown in Fig. 3,

$$\kappa = \kappa(0) \left(\frac{0.1365}{0.1365 - x} \right). \quad (8)$$

The high-concentration limit to these data was set by the fact that all samples fabricated with $x > 0.17$ showed temperature-independent (metallic) resistivity. Equation (6) indicates the dielectric constant κ of thin-film $\text{Ge}_{1-x}\text{Au}_x$ diverges with the critical exponent $\mu = 1$ as has been reported for the Si:P system.¹⁶⁻¹⁸

It is also interesting to see that κ starts to increase significantly when x reaches 0.1, near the value at which Dodson¹⁹ predicted the metal-insulator transition of amorphous GeAu thin films to occur. However, our samples did not show metallic behavior until $x > 0.17$. This was also reported by Edwards *et al.*²⁰

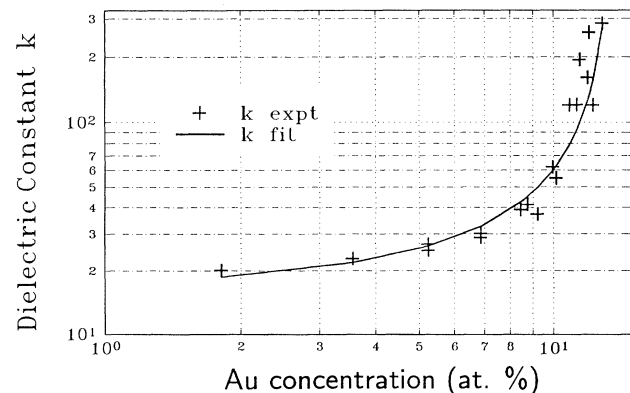


FIG. 3. The dielectric constant κ as a function of Au concentration. The smooth fitting curve indicates that the critical exponent $\mu = 1$ discussed in the text [see Eq. (8)].

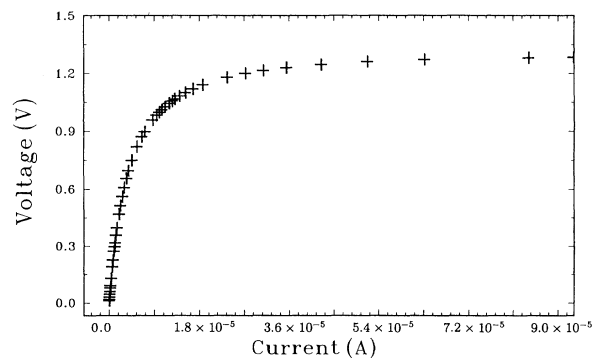


FIG. 4. A typical voltage-current relation for a thin-film GeAu sample at 1.5 K.

B. Theory of field-induced nonlinearity

Figure 4 (Fig. 5) shows I/V characteristics for the present devices at 1.5 K (0.025 K). The previous subsection discussed the resistivity in the steep, linear regions at very low bias. The present section is concerned with understanding the strongly nonlinear features of these curves at higher bias.

Nonlinearity in the I/V characteristic is expected for any type of thermistor, due at least in part to Joule heating by the bias current. This self-heating, in conjunction with the finite thermal conductivity to the temperature bath, causes the strongly biased sample to stabilize at an elevated temperature that depends on the applied bias power.²¹

However, due to the critical energy matching condition in the VRH process and the possibility of inelastic hopping transitions in which phonons participate, an applied bias electric field may also produce nonlinear effects of nonthermal origin.

Field-induced nonlinearity was originally discussed by Hill.²² Later on Pollak^{23,24} treated the problem using percolation theory. Rosenbaum *et al.*²⁵ checked this model experimentally at a few hundred milli-Kelvin. Experiments were also performed on NTD-Ge by Wang *et al.*¹⁰ at temperatures near 20 mK.

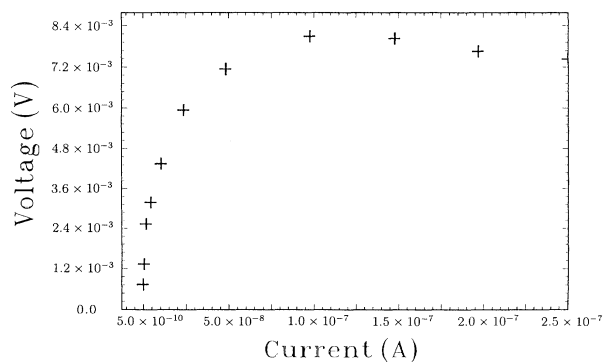


FIG. 5. A typical voltage-current relation for a thin-film GeAu sample at 25 mK.

Including the effect of the electron energy shift due to the bias field in the energy matching condition for hopping leads to a hopping exponent

$$\xi = \frac{2r}{a} + \frac{\epsilon - e\mathbf{E} \cdot \mathbf{r}}{k_b T}, \quad (9)$$

where the bias field enters linearly. This reduces to the exponent of Eq. (3) in the zero-field limit.

Equation (7) has previously been claimed to lead to a resistivity that varied according to²⁵

$$\rho(T, \mathbf{E}) \propto \rho(T, \mathbf{E} = 0) \exp\left(-\frac{eEL}{k_b T}\right), \quad (10)$$

where L is a characteristic hopping length (assumed independent of electric field), and E is the applied electric field. For low field $E < E_c = k_b T / eL$, the constant of proportionality is approximately equal to unity, so that we can write

$$\rho(T, \mathbf{E}) = \rho(T, \mathbf{E} = 0) \exp\left(-\frac{eEL}{k_b T}\right). \quad (11)$$

Various predictions for the temperature dependence of L have been given in the literature. Often $L = CR$ with $C = 0.75$ (Hill) or 0.17 (Pollak and Riess) is used, with R the so-called maximum hopping length.⁶ Shklovskii²⁶ gave $L \approx R^2/a$ with $R = (a/2)(T^*/T)^{1/2}$. These expressions all give dependences of the form $L = pa(T^*/T)^q$, with the constant p ranging from $1/4$ to $1/16$ and q equal to 1 or $1/2$.

IV. OPTIMIZATION OF THE FIELD-ASSISTED HOPPING

Actually Eq. (10) or Eq. (11) is only a very rough approximation, because they are derived without Mott's optimization. Minimization of the tunneling exponent of Eq. (7) with respect to r gives an optimized tunneling exponent, from which the resistance can be calculated by the method given in Ref. 13. The optimized resistivity is found to be

$$\rho(T, \mathbf{E}) = \rho_0(\mathbf{E} = 0) \exp\sqrt{\frac{T^*(\mathbf{E} = 0)}{T} \left(1 - \frac{eEa}{2k_b T}\right)}. \quad (12)$$

The mathematical limit of validity of this expression is $eEa/2k_b T < 1$, which naturally gives the critical field $E_c = 2k_B T / ea$. At higher electric fields, the conduction is expected to be field dominated rather than thermally activated, giving rise to temperature-independent resistivity (activationless hopping).²⁷⁻²⁹ The fields applied in the present work were well below this limit.

It is in fact possible to write Eq. (12) in the form of Eq. (10), obtaining an expression for the field and temperature dependence of the effective length L . The result is

$$L = \frac{4r_{\text{opt}}}{a} \frac{1 - \sqrt{1 - eEa/2k_b T}}{eE/k_b T}. \quad (13)$$

In the zero-field limit this reduces to

$$L = r_{\text{opt}} = \frac{a}{4} \sqrt{\frac{T^*}{T}} \quad (14)$$

which is only dependent on temperature and the properties of the material, as predicted by the nonoptimized theories.

V. EXPERIMENTAL RESULTS ON FIELD-INDUCED NONLINEARITY

To study the effects of bias separately from self-heating, measurements must be made at a given device temperature both with and without applied bias. Decoupling of the electron temperature from the phonon temperature is ignored in this analysis, although such hot electron effects are an alternative way to analyze the nonlinearity (see below).

In the present work, the method of split samples previously described by Wang³⁰ was used to separate the effects of heating and bias field. Two identical, electrically independent thermistor structures were fabricated adjacent to one another on the same $6 \times 6 \text{ mm}^2$ die. The dual device was glued to a copper-clad PC board sample holder. Resistance-temperature curves were obtained for both thermistors in the zero-bias limit by controlling the sample holder temperature, using a metal film heater resistor and calibrated germanium resistance thermometer also mounted on the copper cladding. These low-bias measurements gave $R(T, \mathbf{E} \doteq 0)$ curves for each sample. In a second set of measurements, a power dissipation vs die temperature relation was obtained. This was done by dissipating a known bias power in one of the thermistors and measuring the resistance of the second device at very low bias. (More precisely, the second device in this procedure measures the substrate phonon temperature.) The difference between the resistance measured for the first (high-bias) device and that expected from its zero-bias $R(T)$ relation at the temperature indicated by the second device, gives a measure of the bias-induced nonlinearity.

The importance of the bias-induced nonlinearity can be seen from Figs. 6 and 7. The figures compare the low-bias $R(T, \mathbf{E} = 0)$ and the finite-bias $R(T, \mathbf{E})$ curves for several devices. Here $R(T, \mathbf{E})$ is the resistance measured for a device subjected to bias field \mathbf{E} at a given substrate phonon temperature. $R(T, \mathbf{E} = 0)$ is the resistance at zero bias, but at the substrate temperature known to be produced by the bias power dissipated in the finite-bias $R(T, \mathbf{E})$ measurement. The difference of the two curves in each figure shows the importance of bias-induced nonlinearity. (This plot assumes that the substrate temperature is homogeneous, which is consistent with our measurements, and also ignores electron-phonon decoupling³⁰).

The comparison of the various models [Eqs. (9) and

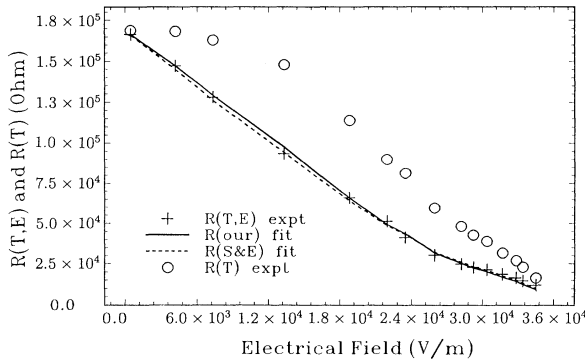


FIG. 6. Bias-induced nonlinearity and the comparison of the various models at bath temperature 1.5 K. Filled circles are the present experimental data for $R(T, E)$, open triangles are the present optimized hopping model [Eq. (11)], plusses are the form of Refs. 26 and 29 with p arbitrarily set to $1/40$, and open circles are the present experimental data for $R(T, E = 0)$ (see text).

(11)] with the observed nonlinearity is also shown in Figs. 6 and 7. Using $L = pa(T^*/T)^q$ with $p = 1/4$, $q = 1$ in Eq. (9) gives a curve (not shown) already an order of magnitude below the data at 4000 V/m. This corresponds to the relations given in Refs. 29 and 30; $L = R^2/a$ and $R = a/2(T^*/T)^{1/2}$. The best fit for $q=1$ is obtained for p arbitrarily set to $1/40$, giving the dash-plusses curves in Figs. 6 and 7. However, particularly at the lowest temperatures, our optimized electric-field-induced hopping prediction [Eq. (11)] explains the data rather accurately. This corresponds to the case $p=1/4$, $q=1/2$ in the low-field limit, but includes explicit field dependence as soon as $E \ll 2k_bT/ea$ is violated. It is clearly shown that one has to assume that L depends not only on temperature, but also on the electrical field as described by Eq. (12) to explain the experimental results quantitatively.

The alternative popular explanation of bias-induced nonlinear resistivity is based on the concept of the decoupling of electron temperature (driven by the bias power dissipation) from the phonon temperature of the substrate. This model has been shown to explain the behavior of NTD-Ge,^{30,31} and it can also account for the behavior of the samples used in this work.³² Further measurements are needed to distinguish between these alternative models.

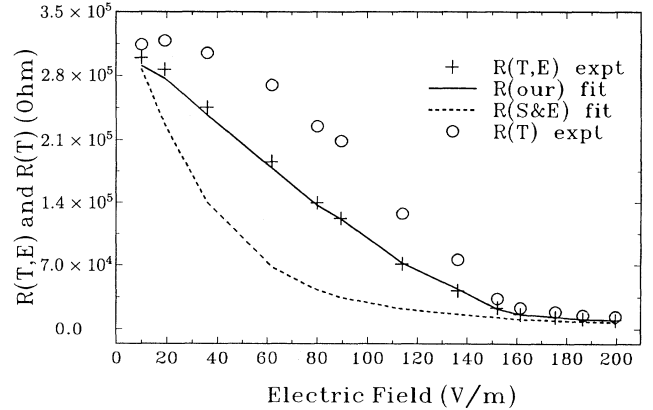


FIG. 7. Bias-induced nonlinearity and the comparison of the various models at bath temperature 25 mK. Curves are as in Fig. 6.

VI. CONCLUSIONS

This has been a study of nonlinear resistivity in thin films exhibiting VRHC. The present work shows that the theory of Shklovskii and Efros can account quantitatively for the temperature and Au concentration dependence of resistance in these films in the limit of zero bias. The prediction of Mott that the dielectric constant κ diverges as the metal-insulator transition is approached from the insulator (VRHC) side, has also been verified here.

A treatment of electric-field-induced nonlinearity in VRHC has been given here which included the effects of hopping optimization as introduced by Mott. The resulting expression for $\rho(T, \mathbf{E})$ qualitatively reproduces the observed nonlinear resistivity, unlike the nonoptimized relation used in previous work.

In future work we hope to make measurements that will definitively distinguish between the various models of bias-induced nonlinearity, and develop a unified and physically correct treatment of the resistivity of these useful and interesting compounds.

ACKNOWLEDGMENTS

This work was supported by the Center for Particle Astrophysics, University of California at Berkeley, National Science Foundation, Subcontract No. 22310NM-6, and by Temple University.

¹ B.I. Shklovskii and A.L. Efros, *Electronic Properties of Doped Semiconductors* (Springer-Verlag, Berlin, 1984).

² H. Tokumoto, R. Mansfield, and M.J. Lea, *Solid State Commun.* **35**, 961 (1980).

³ W.N. Shafarman, D.W. Koon, and T.G. Castner, *Phys. Rev. B* **40**, 1216 (1989).

⁴ N. F. Mott, *J. Non-Cryst. Solids* **8-10**, 1 (1972).

⁵ B. Neuhauser *et al.*, *Jpn. J. Appl. Phys.* **26**, CQ18 (1987).

⁶ S.M. Grannan, A.E. Lange, E.E. Haller, and J.W. Beeman, *Phys. Rev.* **45**, 4516 (1992).

⁷ G. Biskupski, *Philos. Mag. B* **65**, 723 (1992).

⁸ H. Hamimura and A. Kurobe, in *Physics of Disordered Materials*, edited by D. Adler, H. Fritzsche, and S.R. Ovshinsky (Plenum Press, New York, 1985), p. 439.

⁹ Lake Shore Cryotronics, Inc., 64 East Walnut St., Westerville, Ohio 43081.

- ¹⁰ N. Wang *et al.*, Phys. Rev. B **41**, 3761 (1990).
- ¹¹ J.R. Primack, D. Sechel, and B. Sadoulet, Ann. Rev. Nucl. Part. Sci. **38**, 751 (1988).
- ¹² P.F. Smith and J.D. Lewin, Phys. Rep. **187**, 203 (1990).
- ¹³ N.F. Mott, Philos. Mag. **19**, 835 (1969).
- ¹⁴ A. Miller and E. Abrahams, Phys. Rev. **120**, 745 (1960).
- ¹⁵ B. Neuhauser (private communication).
- ¹⁶ N.F. Mott, *Metal-Insulator Transitions*, 2nd ed. (Taylor & Francis, Inc., London, 1990).
- ¹⁷ H. Overhof, *Festkörperprobleme/Advances in Solid State Physics* (Viewig, Braunschweig, 1976), Vol. 16, p. 239.
- ¹⁸ M.A. Paalanen, T.F. Rosenbaum, G.A. Thomas, and R.N. Bhatt, Phys. Rev. Lett. **51**, 1896 (1983).
- ¹⁹ B.W. Dodson, W.L. McMillan, and J.M. Mochel, Phys. Rev. Lett. **46**, 46 (1981).
- ²⁰ A.M. Edwards, M.C. Fairbanks, and R.J. Newport, Philos. Mag. B. **63**, 457 (1991).
- ²¹ A. Madan and M.P. Shaw, *The Physics and Applications of Amorphous Semiconductors* (Academic Press, Orlando, 1988).
- ²² R.M. Hill, Philos. Mag. **24**, 1307 (1971).
- ²³ M. Pollak, J. Non-Cryst. Solids **11**, 1 (1972).
- ²⁴ M. Pollak and I. Riess, J. Phys. C **9**, 2339 (1976).
- ²⁵ T.F. Rosenbaum, K. Andres, and G.A. Thomas, Solid State Commun. **35**, 663 (1980).
- ²⁶ B.I. Shklovskii, Fiz. Tekh. Poluprovodn. **10**, 1440 (1976) [Sov. Phys. Semicond. **10**, 855 (1976)].
- ²⁷ O. Fraran and Z. Ovadyahu, Solid State Commu. **67**, 823 (1988).
- ²⁸ D. Shahar and Z. Ovadyahu, Phys. Rev. Lett. **64**, 2293 (1990).
- ²⁹ F. Tremblay, M. Pepper, R. Newbury, D. Ritchie, and D.C. Peacock, Phys. Rev. B **40**, 3387 (1989).
- ³⁰ N. Wang, Ph.D. thesis, University of California at Berkeley, 1991.
- ³¹ T.A. Shutt, Ph.D. thesis, University of California at Berkeley, 1993.
- ³² X.X. Wang, C.J. Martoff, and E. Kaczanowiz, J. Low Temp. Phys. **93**, 349 (1993).